Research Article

Cancer Prevention Research

Epigenetic DNA Methylation of Antioxidative Stress Regulator *NRF2* in Human Prostate Cancer

Tin Oo Khor[1], Francisco Fuentes[1], Limin Shu[1], Ximena Paredes-Gonzalez[1], Anne Yuqing Yang[1], Yue Liu[2], Dominic J. Smiraglia[3], Srinivasan Yegnasubramanian[4], William G. Nelson[4], and Ah-Ng Tony Kong[1]

Abstract

Epigenetic control of *NRF2*, a master regulator of many critical antioxidative stress defense genes in human prostate cancer (CaP), is unknown. Our previous animal study found decreased Nrf2 expression through promoter CpG methylation/histone modifications during prostate cancer progression in TRAMP mice. In this study, we evaluated CpG methylation of human *NRF2* promoter in 27 clinical prostate cancer samples and in LNCaP cells using MAQMA analysis and bisulfite genomic DNA sequencing. Prostate cancer tissue microarray (TMA) containing normal and prostate cancer tissues was studied by immunohistochemistry. Luciferase reporter assay using specific human *NRF2* DNA promoter segments and chromatin immunoprecipitation (ChIP) assay against histone modifying proteins were performed in LNCaP cells. Three specific CpG sites in the NRF2 promoter were found to be hypermethylated in clinical prostate cancer samples (BPH<ADT-RCaP<AS-CaP). NRF2 staining in human prostate cancer TMA showed a decreasing trend for both intensity and percentage of positive cells from normal tissues to advanced-stage prostate cancer (Gleason score from 3–9). Reporter assays in the LNCaP cells containing these three CpG sites showed methylation-inhibited transcriptional activity of the *NRF2* promoter. LNCaP cells treated with 5-aza/TSA restored the expression of NRF2 and NRF2 downstream target genes, decreased expression levels of DNMT and HDAC proteins, and ChIP assays showed increased RNA Pol II and H3Ac with a concomitant decrease in H3K9me3, MBD2, and MeCP2 at CpG sites of human *NRF2* promoter. Taken together, these findings suggest that epigenetic modification may contribute to the regulation of transcription activity of *NRF2*, which could be used as prevention and treatment target of human prostate cancer. *Cancer Prev Res; 7(12); 1186–97. ©2014 AACR.*

Introduction

In the United States, prostate cancer (CaP) is the most commonly diagnosed non–skin cancer and the second leading cause of cancer-related deaths (1). In 2014, it is estimated that 233,000 men will be diagnosed with the disease and 29,480 will die (2). Prostate cancer is one of the most complicated human tumors, and similar to many other malignancies, it arises from progressive genetic and epigenetic alterations, which rapidly change these tumors from a clinically benign state to a malignant one (3, 4). Epigenetic alterations can largely contribute to the malignant transformation and progression of prostate cancer through the deregulation of many genes involved in critical cellular processes, including DNA-damage repair (e.g., *GSTP1*, *GSTM1*, and *MGMT*), hormonal responses (e.g., *AR*, *ERα*, *ERβ*, and *RARβ*), tumor suppression (e.g., *KAI1*, *factor-β*, and *DAB2IP*), tumor-cell invasion/metastasis (e.g., *CDH1* and *CD44*), apoptosis (e.g., *SLC18A2* and *TNFRSF10C*), and cell-cycle control (e.g., *CDKN2A*/*p16* and *RASSF1A*; refs. 5, 6). Therefore, the deregulation of the antioxidant defense system has been gaining increased attention because it promotes toxicity and the neoplastic progression of prostate cancer (4, 7, 8).

Erythroid 2p45 (NF-E2)–related factor 2 (NRF2) is a basic-region leucine zipper (bZIP) transcription factor that regulates the expression of many phase II detoxifying/antioxidant enzymes, such as glutathione *S*-transferase (GST), UDP-glucuronosyltransferase (UGT), heme oxygenase-1 (HO-1), NADP(H):quinone oxidoreductase (NQO), glutamate cysteine ligase (GCL), and γ-glutamylcysteine synthetase (γGCS), by binding in combination with small Maf

[1]Department of Pharmaceutics, Ernest Mario School of Pharmacy, Rutgers, The State University of New Jersey, Piscataway, New Jersey. [2]Department of Chemical Biology, Susan Lehman Cullman Laboratory for Cancer Research, Ernest Mario School of Pharmacy, Rutgers, The State University of New Jersey, Piscataway, New Jersey. [3]Department of Cancer Genetics, Roswell Park Cancer Institute, Buffalo, New York. [4]Sidney Kimmel Comprehensive Cancer Center, Johns Hopkins University, Baltimore, Maryland.

Note: Supplementary data for this article are available at Cancer Prevention Research Online (http://cancerprevres.aacrjournals.org/).

Corresponding Author: Ah-Ng Tony Kong, Center for Cancer Prevention Research, Department of Pharmaceutics, Ernest Mario School of Pharmacy, Rutgers, The State University of New Jersey, 160 Frelinghuysen Road, Piscataway, NJ 08854. Phone: 732-455-3831; Fax: 732-455-3134; E-mail: KongT@pharmacy.rutgers.edu

doi: 10.1158/1940-6207.CAPR-14-0127

proteins to antioxidant response elements (ARE) in promoter regions (9). Thus, NRF2 is cytoprotective by reducing the toxicity of reactive intermediates, which protects against oxidative or electrophilic challenges and maintains cellular chemical homeostasis (10, 11). *In vivo*, NRF2 is dispensable for mouse growth and development (12). Accordingly, *Nrf2*-deficient ($Nrf2^{-/-}$) mice have been demonstrated to markedly exhibit lower expression levels of cellular defense genes in various tissues (4, 13). These mice are inherently more susceptible to oxidative stress-induced diseases and chemically induced DNA damage, which increases their risk of developing certain types of cancer (e.g., stomach, colorectal, and skin) compared with wild-type mice (14–19).

Diverse studies have shown that the levels of NRF2 and members of the GST mu family are decreased in human prostate cancer (20). Recently, the expression of NRF2 in prostate tumors from TRAMP mice was shown to be suppressed epigenetically by promoter CpG methylation and histone modifications in association with MBD2 (8). Interestingly, the treatment of TRAMP C1 cells with the DNA methyltransferase (DNMT) inhibitor 5-aza-2′-deoxycytidine (5-aza) and the histone deacetylase (HDAC) inhibitor trichostatin A (TSA) restored NRF2 expression, representing a promising approach to treating cancer by reversing epigenetic modifications and increasing the expression of NRF2 and its downstream antioxidant and detoxification enzymes (8, 21). Similarly, absent or reduced GSTP1 expression has also been reported in high-grade prostate intraepithelial neoplasias, and methylation of its promoter has been the most frequently detected epigenetic alteration, which occurs in more than 90% of cancer samples and approximately 70% of prostate intraepithelial neoplasia samples (22). In contrast, the loss of GSTP1 is rarely detected in normal prostate or benign prostatic hyperplasia (BPH) tissues (5). Furthermore, the expression and activity of SOD, catalase, and GPx are decreased in prostate cancer tissues, plasma, and erythrocytes (23, 24). Taken together, these studies confirm the pivotal role of NRF2 and its target genes in controlling oxidative stress and chronic inflammatory processes in prostate cancer and the epigenetic mechanisms involved in its regulation.

Materials and Methods

Reagent and cell culture

All the enzymes used in this study were obtained from New England Biolabs Inc. The Dual-Luciferase Assay system and the luciferase reporter vectors pGL 4.75 with cytomegalovirus (CMV) promoter and pGL 4.15 were obtained from Promega. All other chemicals, including dimethyl sulfoxide (DMSO), 5-aza, and TSA, were purchased from Sigma. LNCaP (androgen-dependent prostate cancer cell line from the American Type Culture Collection) cells were maintained in RPMI-1640 with 10% fetal bovine serum (FBS; Gibco) and grown at 37°C in a humidified 5% CO_2 atmosphere. Cells were cytogenetically tested and authenticated before being frozen. Cell line was used no longer than 6 months after resuscitation from freezing. The LNCaP cells were plated on 10-cm plates for 24 hours and then treated with 0.1% DMSO or 2.5 μmol/L 5-aza with 1% FBS-containing medium. The medium was changed every 2 days. For the 5-aza and TSA combination treatment, 500 nmol/L TSA was added to the 5-aza–containing medium on the day 6 and cultured for another 24 hours. The cells were then harvested for DNA, RNA, and protein analyses.

Human prostate tissue samples

BPH samples ($n = 9$) were obtained from patients treated for lower urinary tract symptoms by transurethral prostatectomy. Androgen-stimulated prostate cancer (AS-CaP) samples ($n = 7$) were obtained from patients treated for prostate cancer by prostatectomy. Androgen-deprivation therapy recurrent prostate cancer (ADT-RCaP) tumor samples ($n = 11$) were obtained by transurethral resection from patients who presented urinary retention from recurrent prostate cancer during ADT-RCaP (25). All samples were obtained from the Roswell Park Cancer Institute (Buffalo, NY). AS-CaP and BPH were enriched to >70% epithelial cells using the standard microdissection of 20-μm frozen step sections adjacent to 8-μm sections identified by H&E staining, which contained >50% epithelial cells as previously described by Berthon and colleagues (26). ADT-RCaP did not require microdissection as it was, on average, composed of 92% malignant cells (25).

MassARRAY quantitative methylation analysis

MassARRAY quantitative methylation analysis (MAQMA) was performed to interrogate the methylation levels of the *NRF2* promoter (Supplementary Fig. S1) in human prostate tissue samples using the MassARRAY Compact system and EpiTYPER software (Sequenom) as previously described (27). Genomic DNA was isolated using the DNeasy Tissue Kit (Qiagen) and subjected to bisulfite conversion. The bisulfite conversion was performed using 750 ng of genomic DNA with the EZ DNA Methylation Gold Kit (Zymo Research Corp.) following the manufacturer's instructions. The CpG sites identified in the 5′-flanking region of human *NRF2* gene spanning from position −1552 to +1091 were analyzed using eight locus-specific amplicons (Fig. 1A). The primer sequences used to amplify the converted DNA are described in Supplementary Table S1.

Bisulfite Genomic Sequencing

Genomic DNA and sodium bisulfite converted genomic DNA from prostate tissue samples and DMSO- or 5-aza/TSA–treated LNCaP cells were obtained using the same procedures as described above. The converted DNA was amplified by PCR using Platinum PCR SuperMix (Invitrogen) with three specific sets of bisulfite genomic sequencing (BGS) primers spanning three differentially methylated CpG sites from −1530 to −1143, with the translational start site (TSS) referenced as +1 (Supplementary Table S1). The primers were designed using MethPrimer (28). The following PCR amplification conditions were used: 3 minutes at 94°C; 30 seconds at 94°C, 45 seconds at 70/55°C and

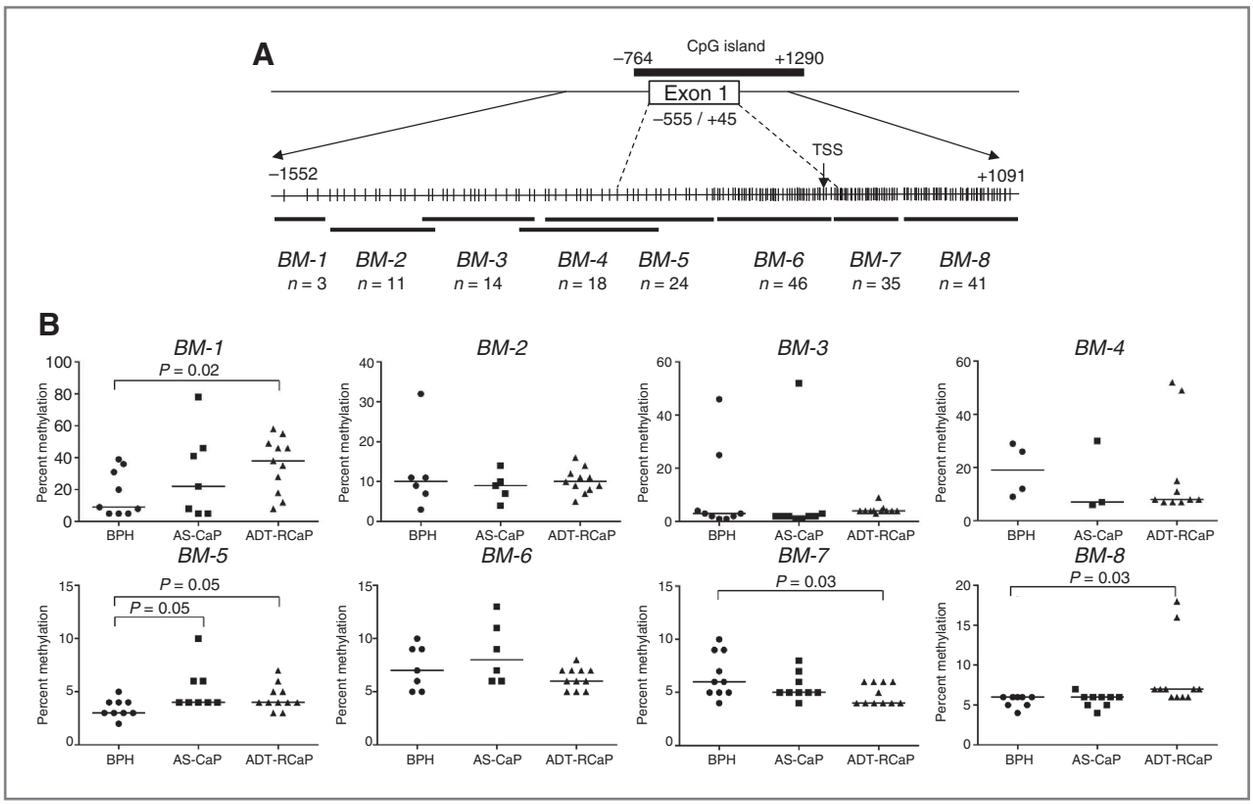

Figure 1. Hypermethylation of three specific CpG sites in the *NRF2* promoter were differentially methylated in human prostate tissues by MAQMA analysis. A, sequence of *NRF2* promoter covered by MAQMA analysis is schematically represented with CpG sites indicated by vertical lines. CpG sites were identified in the 5′-flanking region of human *NRF2* gene spanning from position −1552 to +1091. The primer sequences used to amplify the converted DNA are described in Supplementary Table S1. B, locus-specific DNA methylation of *NRF2* promoter in human BPH, AS-CaP, and ADT-RCaP tissues was determined by MAQMA analysis as described in Materials and Methods. Each symbol represents an individual sample and the bar indicates the median of each group.

1 minute at 72°C for 15 cycles; 30 seconds at 94°C, 45 seconds at 60°C and 1 minute at 72°C for 25 cycles; and 5 minutes at 72°C for 1 cycle. The PCR products were cloned into the pCR4 TOPO vector using a TOPO TA Cloning Kit (Invitrogen). Plasmid DNA from at least 10 colonies from each treatment was prepared using the QIAprep Spin Miniprep Kit (Qiagen) and sequenced (Genwiz; ref. 29).

Immunohistochemistry

Immunohistochemical (IHC) staining was performed on a high-density prostate cancer tissue microarray (TMA) containing 27 tissue cores of normal prostate tissue and 160 tissue cores of prostate cancer tissue including adjacent tissue (hyperplasia) and adenocarcinoma tissue with Gleason score from 3–9 from BioMax Company. IHC staining was performed as described previously (30), using primary antibodies directed against NRF2 (1:100 dilution). The results of the IHC analysis (accumulated immunostaining intensity and percentage of positive cells) were determined by using an IHC Image Analysis algorithm to detect both cytoplasmic and nuclei staining using an Aperio ScanScopeR GL system (Aperio Technologies). The NRF2 immunostaining results were scored according to the accumulated intensity as 0, negative; 1+, weak; 2+, moderate; or 3+, strong. All images were quality controlled for accuracy of the tissue recognition software, in addition to accuracy of the image analysis algorithm.

Plasmids

The genomic sequence of the human *NRF2* promoter region was retrieved from the human NCBI genome database. Two human *NRF2* promoter segments, −1526-1 and −1169-1 (with the TSS referred to as position +1), were amplified from human genomic DNA isolated from normal human prostate cells using the following primers: 1526 forward, 5′-GGTACCACCTAGAGAAAGTAAGCTCTGC-3′; 1169 forward, 5′-GGTACCCATACTTGGAAGTAACAAGGAG-3′; and a common reverse primer, 5′-CTCGAGATGAGCTGTGGACCGTGTGTT-3′. The PCR products were cloned into the pCR4 TOPO vector using a TOPO TA Cloning kit (Invitrogen), digested with *Kpn*I and *Xho*I and then inserted into the pGL4.15 luc2P/Hygro vector. All the recombinant plasmid sequences were verified by sequencing (Genwiz). The CpG-methylated reporters were generated by treating the reporter plasmids with methyltransferase M.SssI according to the manufacturer's instructions. Briefly, 5 mg of the reporter constructs were incubated with 5 U of M.SssI for 1 hour in NEBuffer 2 (50 mmol/L

NaCl, 10 mmol/L Tris–HCl pH 7.9, 10 mmol/L $MgCl_2$, and 1 mmol/L dithiothreitol) supplemented with 160 mmol/L S-adenosylmethionine at 37°C. Methylated plasmids were purified using the QIAquick PCR Purification Kit (Qiagen), and the concentrations of all plasmids were determined by agarose gel electrophoresis. The efficiency of the methylation reactions was confirmed by digestion using the methylation-dependent *Hha*I and *Hpa*II restriction endonucleases.

Transfection and luciferase reporter assay

LNCaP cells were plated in 12-well plates for 24 hours and then transfected with 500 ng of the indicated reporter plasmids with GeneJuice (Novagen) according to the manufacturer's instructions. A total of 750 ng of pGL 4.75, which contains a β-galactosidase gene driven by a CMV promoter, was cotransfected as an internal control. After 24 hours of transfection, the cells were lysed in a Dual-Luciferase lysis buffer, and 10-mL aliquots of the cell lysate were assayed using the Dual-Luciferase Assay Kit with a Sirius luminometer (Berthold Technologies). The transcriptional activities of each construct were calculated by normalizing the firefly luciferase activities with the corresponding β-galactosidase enzyme activities and were reported as the fold change in induction relative to the empty pGL 4.15 vector. The values are expressed as the mean ± SD of four separate samples.

RNA isolation and reverse transcription PCR

Total RNA was extracted from the treated cells using the RNeasy Mini Kit (Qiagen). First-strand cDNA was synthesized from 1 μg of total RNA using the SuperScript III First-Strand Synthesis System for RT-PCR (Invitrogen) according to the manufacturer's instructions. The cDNA was used as the template for real-time PCR (Applied Biosystems ViiA 7 Real-Time PCR System). The sequences of the primers used for cDNA amplification are described in Supplementary Table S1.

Preparation of protein lyses and Western blotting

The treated cells were harvested using radioimmunoprecipitation assay (RIPA) buffer supplemented with a protein inhibitor cocktail (Sigma). The protein concentrations of the cleared lysates were determined using the bicinchoninic acid (BCA) method (Pierce), and 20 mg of the total protein was resolved by 4% to 15% SDS-PAGE (Bio-Rad). After electrophoresis, the proteins were electro-transferred to a polyvinylidene difluoride (PVDF) membrane (Millipore). The PVDF membrane was then blocked with 5% BSA in PBS-0.1% Tween 20 (PBST) and then sequentially incubated with specific primary antibodies and horseradish peroxidase (HRP)–conjugated secondary antibodies. The blots were visualized with the Super Signal enhanced chemiluminescence (ECL) detection system and documented using the Gel Documentation 2000 system (Bio-Rad). The antibodies were purchased from the following sources: anti-NRF2 from Epitomics Inc.; anti-NQO1, anti-HO1, and anti-β-actin from Santa Cruz Biotechnology; anti-DNTM1, anti-DNMT3a, and anti-DNMT3b from IMGENEX; and anti-HDAC 1–6 from Cell Signaling Technology.

Chromatin immunoprecipitation assay

The chromatin immunoprecipitation (ChIP) assays were performed using the MAGnify Chromatin Immunoprecipitation System (Invitrogen) following the manufacturer's instructions. Briefly, LNCaP cells treated with DMSO or 5-aza/TSA for 7 days were washed with PBS and trypsinized. The trypsinized cells were then washed with PBS, and the chromatin from the cells (100,000 cells were used per IP) was cross-linked with 1% formaldehyde for 10 minutes at room temperature and sonicated to generate approximately 200- to 500-bp DNA fragments in lysis buffer. The proteins were then immunoprecipitated with 6 to 10 μL of anti-Pol II, anti-MBD2, anti-MeCP2, anti-trimethyl-histone H3-Lys9 (H3K9me3), and anti-H3Ac antibodies (Millipore) or mouse IgG to capture DNA-bound protein complexes. The enrichment of the eluted DNA was quantified by comparison with the input lysate by qPCR (29) using designed primers covering a 93-bp fragment that is 29 bp upstream of the first CpG site in the *NRF2* promoter (Supplementary Table S1).

Statistical analysis

All experiments were performed at least three times with similar results. Differences in the DNA methylation levels between paired samples were analyzed using the Student *t* test with the Welch correction factor; the data for the luciferase reporter assay transcriptional activity, mRNA expression, ChIP assay, and percentage of IHC-positive cells were evaluated using the Student *t* test. A linear regression analysis was used to correlate the accumulated intensity of IHC of NRF2 and tissue groups (normal, hyperplasia, and adenocarcinoma tissue with Gleason score from 3–9). All *P* values were two-sided, and a *P* value of <0.05 was considered to be statistically significant.

Results

Methylation of specific CpG sites in the *NRF2* promoter was differentially methylated in advanced stages of human prostate cancer

The genomic sequence of the *NRF2* gene (NC_000002.11: 178095031-178129859, *Homo sapiens* chromosome 2, reference GRCh37.p10 primary assembly, including 2.1 kb of its 5′-upstream sequence) was analyzed for CpG islands using the CpG Island Searcher (31). For simplicity, the distal boundary of the TSS (ATG) is defined as position +1. The CpG island of human NRF2 was identified between −764 and +1290 with a GC content of 66.6%, a CpG observed:expected ratio of 0.85 and a total of 205 CpG sites. Thus, the CpG island of the human *NRF2* gene comprised the first exon and part of the first intron (Fig. 1A).

To assess the methylation levels in the *NRF2* promoter across multiple patients, we performed MAQMA analysis of eight locus-specific PCR products from sodium bisulfate–converted DNA spanning position −1552 to +1091

(Fig. 1B; Supplementary Fig. S1). The analysis revealed specific hypermethylation in prostate tumor tissues (AS-CaP and ADT-RCaP, ranging from 5% to 78% methylation) of the *BM-1* locus, which comprised three CpG sites within position −1493 to −1185 (Fig. 1B; $P < 0.05$). Although the analysis also showed significant differences in other specific promoter loci (e.g., the *BM-5* locus), the methylation levels in prostate tumor tissue were low (Fig. 1B). To validate the methylation status of these three specific CpG sites in the *NRF2* promoter, we performed BGS in the same set of human tissue samples. Figure 2A shows that CpG sites were differentially methylated in prostate tumors (AS-CaP and ADT-RCaP; 25.3% and 43.6% methylation, respectively) compared with human BPH tissues (19.6% methylation; $P < 0.05$). In addition, eight downstream CpG sites (−1135 to −917) were examined; however, these sites were poorly methylated (∼2%) and did not display differential methylation levels among the prostate tissues (data not shown).

IHC staining of NRF2 in prostate cancer tissue array exhibited a wide range of intensity

To investigate the NRF2 expression in clinical samples, we examined the levels of NRF2 protein expression on a high-density prostate cancer TMA, using IHC staining against NRF2 protein (Fig. 2B). The analysis revealed that all sections containing normal, hyperplasia, and adenocarcinoma tissues showed positive NRF2 staining (Fig. 2B). Although both nucleus and cytoplasm show positive staining, majority of the NRF2 staining was observed in cytoplasm. The accumulated intensity of IHC staining of NRF2 revealed a

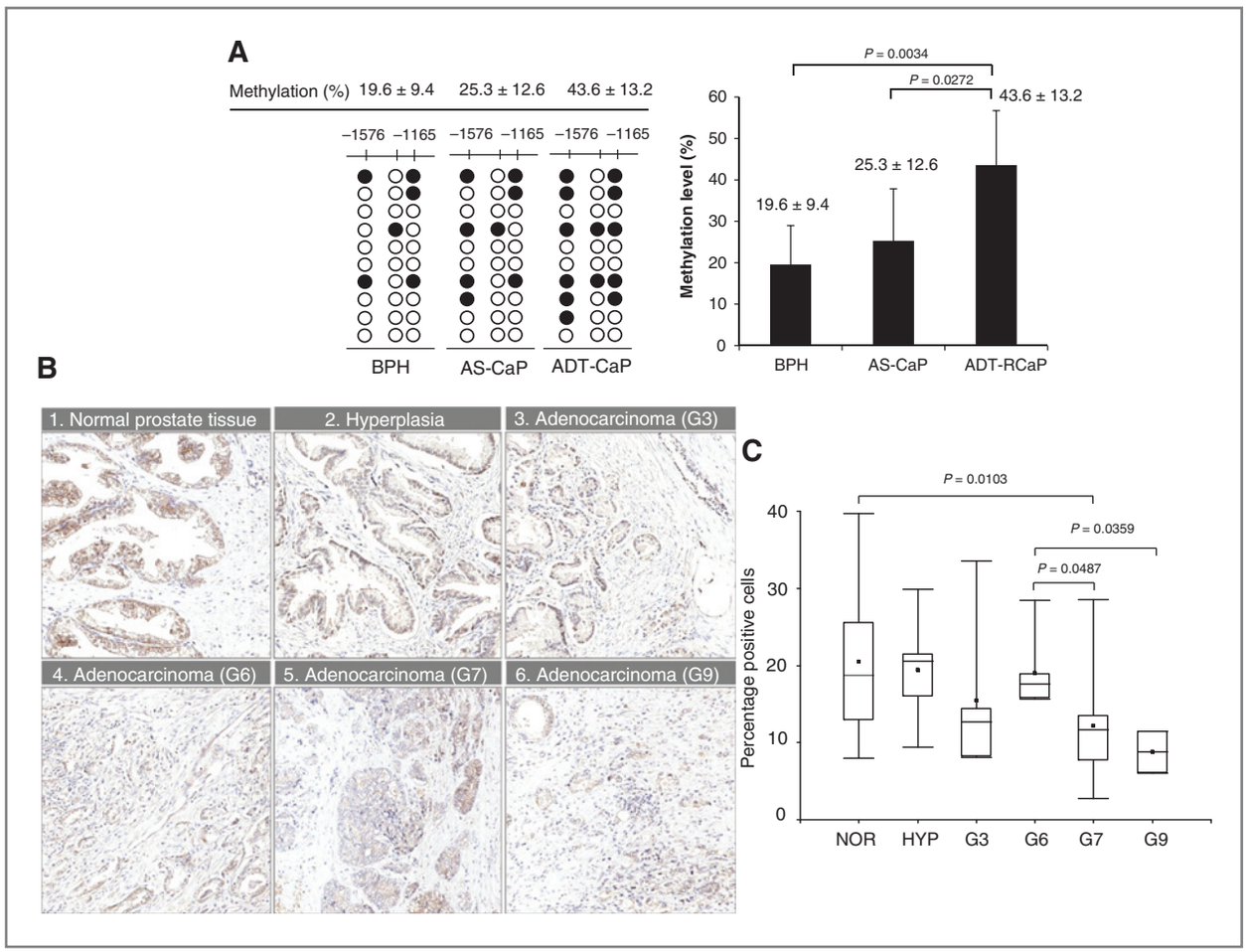

Figure 2. BGS of three CpGs sites of *NRF2* promoter in human prostate tissues and IHC staining of NRF2. A, methylation level of three CpGs sites of *NRF2* promoter in human BPH, AS-CaP, and ADT-RCaP tissues. Plasmid DNA from at least 10 colonies from each sample was prepared using the QIAprep Spin Miniprep Kit (Qiagen) and sequenced (Genwiz). Average methylation value for each tissue type is illustrated using representative white (unmethylated) and black (methylated) dots for each CpG site. Detailed procedure and sequence information are described in Material and Methods. The values are mean ± SD of independent samples for BPH ($n = 9$), AS-CaP ($n = 7$), and ADT-RCaP ($n = 11$). B, normal, hyperplasia, and adenocarcinoma prostate tissues with Gleason score (G) from 3–9, showing differential IHC staining levels of NRF2 (with accumulated intensity value scored as 2+). C, percentage of positive cells (%) showing IHC staining of NRF2 (with accumulated intensity value scored as 2+) in normal (NOR), hyperplasia (HYP), and adenocarcinoma prostate tissues with Gleason score (G) 3–9.

wide range from low to high intensity in all the tissue groups analyzed. As described in the Materials and Methods, the NRF2 immunostaining results, scored according to the accumulated intensity, revealed that the strong staining (with accumulated intensity value scored as 3+) between normal and adenocarcinoma tissues did not show a significant difference ($P = 0.9543$). However, in the moderate staining (with accumulated intensity value scored as 2+), which included 25 tissue cores of normal prostate tissue and 34 tissue cores of prostate cancer tissue (hyperplasia and adenocarcinoma tissues with Gleason score from 3–9), the accumulated intensity of NRF2 staining showed a decreasing trend from normal tissues to advanced-stage prostate cancer (adenocarcinoma tissue with Gleason score from3–9; Fig. 2B). Likewise, the percentage of positive cells showed similar decreasing trend of NRF2 protein expression with significant differences between normal and advanced prostate cancer tissues ($P < 0.05$; Fig. 2C). Furthermore, when comparing adenocarcinoma with its adjacent tissues, we observed that the adjacent benign lumina tissue shows a relatively stronger staining (Fig. 2B).

In vitro methylation of three specific CpGs sites suppressed the transcriptional activity of the human *NRF2* promoter

Because promoter CpG demethylation often appears to regulate the transcriptional activation of genes, we examined the functional role of the three specific CpG sites in LNCaP cells with the pGL4.15-1526 and pGL4.15-1169 luciferase reporters, which contained the *NRF2* promoter with or without the three CpG sites, respectively (Fig. 3A). To confirm the methylation status of both constructs, the reporter plasmids were methylated *in vitro* by M.sssI CpG methyltransferase and then digested with the *Hpa*I or *Hha*II CpG-methylation–sensitive restriction endonucleases (Fig. 3B). When LNCaP cells were transfected with the unmethylated *NRF2* promoter/luciferase reporter plasmids containing the three specific CpG sites, there was a 50-fold increase in luciferase reporter expression. Conversely, when the specific CpG sites were absent, the luciferase reporter expression was significantly decreased by 33-fold (Fig. 3C). The transcriptional activity of the methylated *NRF2* promoters decreased dramatically (to ~1-fold) when the specific CpG sites were present in the promoter. Nevertheless, when the three CpG sites were absent, the luciferase activity was decreased to approximately 2-fold ($P < 0.05$; Fig. 3C). These data suggest that these three CpG sites play a critical role in regulating *NRF2* promoter activity. Similar results were also obtained with PC-3 and HeLa cells (Supplementary Fig. S2).

Methylation of specific CpG sites in the *NRF2* promoter can be reversed in human prostate cell lines with 5-aza/TSA treatment

We previously reported that combined treatment with DNMT and HDAC inhibitors 5-aza and TSA, respectively, decreases the CpG methylation levels of the *NRF2* promoter in murine prostate cancer TRAMP C1 cells (8). Bisulfite sequencing of genomic DNA from LNCaP cells was performed to examine the methylation levels and determine whether 5-aza/TSA treatment decreases *NRF2* promoter methylation. As shown in Fig. 4A, the combined 5-aza/TSA treatment over 7 days in LNCaP cells significantly reduced ($P < 0.05$) the methylation level of these specific CpG sites (−1530 to −1143) from 62.96% to 32.78%. Similar to human prostate tumor samples, the next eight downstream CpG sites (−1166 to −896) were poorly methylated (~1%) and did not show any differential methylation change between DMSO and 5-aza/TSA treatments.

Expression of NRF2 and NRF2-related genes were induced by 5-aza/TSA treatment

To investigate the effect of the 5-aza/TSA treatment on the expression of NRF2 and its related genes in LNCaP cells, we first examined the expression of *NRF2*, *NQO1*, and *HO-1* by real-time RT-PCR. Accordingly, the gene expression levels of *NRF2* and ARE-mediated genes were significantly ($P < 0.05$) increased in the 5-aza/TSA–treated LNCaP cells compared with the control (Fig. 4B). We next assessed the protein levels of NRF2, NQO1, and HO-1 by Western blot analysis. Figure 4C shows that the protein levels from NRF2 and ARE-mediated genes were in agreement with the previous findings as there were increased protein levels compared with those in the 0.1% DMSO-treated control cells.

Expression of DNMTs and HDACs were influenced by 5-aza/TSA treatment

We next examined the protein levels of DNMTs and HDACs in LNCaP cells after the control and 5-aza/TSA treatments because DNA methylation is regulated by DNMTs, including DNMT1, DNMT3a, and DNMT3b, and histone methylation is controlled by the HDAC enzymes (4). Figure 5A shows that the 5-aza/TSA treatment dramatically decreased the protein expression of DNMT1, DNMT3a, and DNMT3b by fold changes of approximately 0.5, 0.6, and 0.3, respectively, compared with the control. As expected, HDAC (1–6) protein expression was also decreased after the 5-aza/TSA treatment (Fig. 5B).

Methylation of specific CpG sites in the *NRF2* promoter was associated with H3-Lys9 (H3K9m3) and histone modification, which can be reversed by 5-aza/TSA treatment

DNA methylation has been widely reported to interact with various methyl-CpG–binding domain proteins (MBD) and methyl CpG binding protein 2 (MeCP2; refs. 32, 33). These binding proteins can then also interact with a corepressor complex that includes HDACs, which results in the transcriptional repression of certain genes (34). ChIP assay analysis was performed using specific H3Ac, Pol II, H3K9Me3, MBD2, and MeCP2 antibodies to investigate the proteins that could be potentially bound to the *NRF2* promoter in control and 5-aza/TSA–treated LNCaP cells. Interestingly, the 5-aza/TSA treatment of LNCaP cells increased the total amount of H3Ac enrichment and further decreased the total amount of H3K9Me3, MBD2, and MeCP2 at the *NRF2* promoter ($P < 0.05$). In agreement

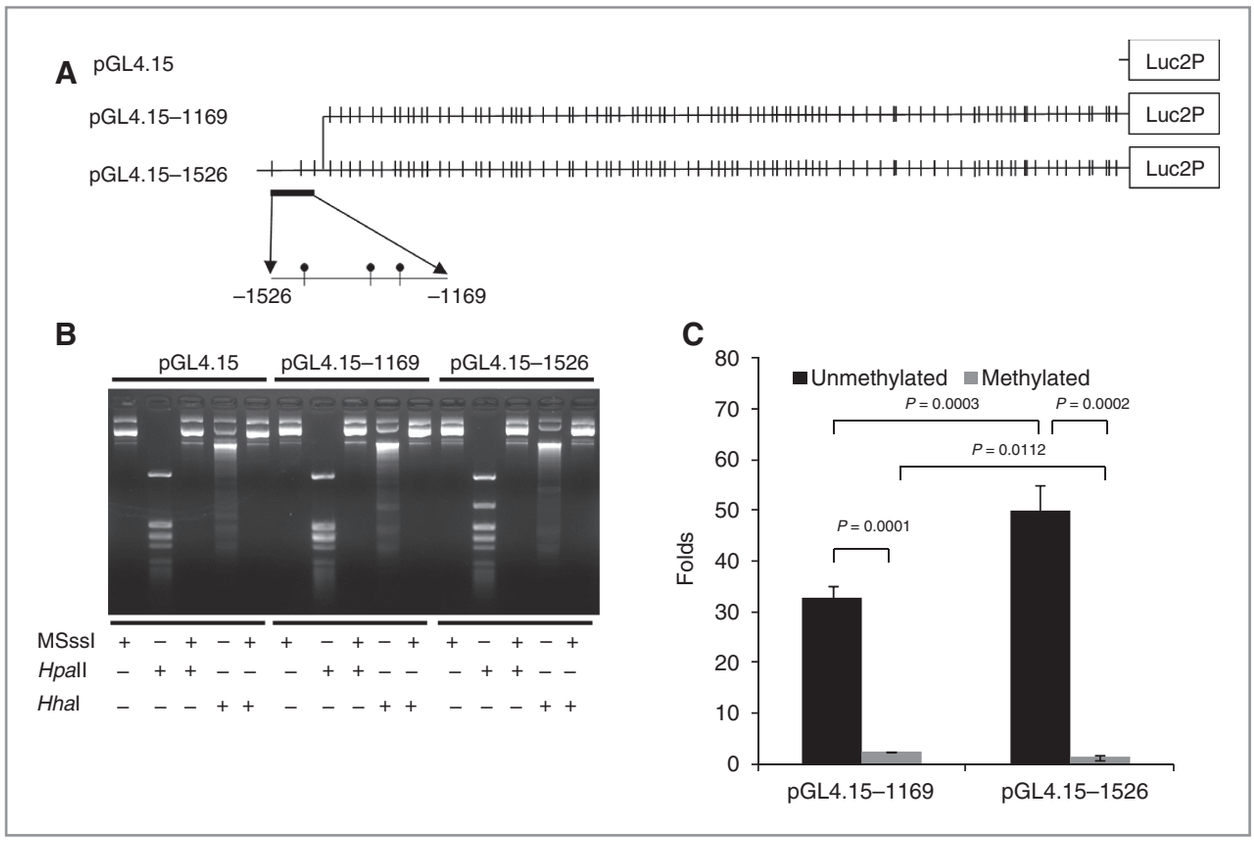

Figure 3. Methylation of three specific CpG sites inhibited the *in vitro* transcriptional activity of *NRF2* promoter. A, the construction of luciferase reporters is schematically represented. *NRF2* promoters with (−1526–1) or without (−1169–1) the extra sequence containing the three specific CpG sites were amplified from human genomic DNA and inserted into pGL 4.15 vector. The resulted reporters were designated as pGL-1526 and pGL-1169, respectively. B, pGL-4.15, pGL-4.15–1169, and pGL-4.15–1526 reporters were methylated *in vitro* by M.sssI CpG methyltransferase, then digested with *Hpa*I or *Hha*II. *Hpa*I and *Hha*II are CpG-methylation–sensitive restriction endonucleases whose activity is blocked by CpG methylation. C, pGL-1526 or pGL-1169 reporters, either methylated by CpG methyltransferase or not, were cotransfected with pGL 4.75 vector that contains a β-galactosidase gene driven by CMV promoter into LNCaP cells, and the luciferase activities were measured after 24 hours. The transcriptional activities of each construct were calculated by normalizing the firefly luciferase activities with the corresponding β-galactosidase enzyme activities and were reported as the fold change in induction relative to the empty pGL 4.15 vector. The values are expressed as the mean ± SD of four separate samples.

with the above results, Pol II was enriched at the *NRF2* promoter ($P < 0.05$), suggesting a suppression of *NRF2* transcription in LNCaP cells basally and that the activation of *NRF2* could be reversed by the 5-aza/TSA treatment (Fig. 6).

Discussion

NRF2 has been widely described as a key transcription factor regulating the activity of many ARE-mediated type II detoxifying/antioxidant enzymes in response to antioxidative/electrophilic stimuli and therapeutic signals (4, 35, 36). In this context, NRF2 has been reported to be downregulated in human prostate cancer and prostate cancer in TRAMP mice, revealing that the loss of NRF2 correlates with the reduced expression of several classes of GSTs, which ultimately leads to elevated ROS levels and the DNA damage that is associated with tumorigenesis (8, 20). Conversely, the aberrant overexpression of NRF2 from gain-of-function mutations or the deregulation of factors regulating NRF2 expression has been detected in various advanced cancer tissues, including lung, esophagus, larynx, gallbladder, skin, pancreas, ovary, and breast (37, 38). Thus, the nuclear accumulation of NRF2 in these cancers leads to higher levels of cytoprotective proteins, including detoxifying/biotransformation enzymes, drug transporters, antioxidants, and antiapoptotic proteins, which results in decreased apoptosis, increased cell survival, and drug resistance to chemotherapy (4, 39).

We have also demonstrated that *NRF2* expression is regulated by an epigenetic mechanism during prostate cancer progression in TRAMP mice *in vivo* and in TRAMP C1 cells *in vitro*, suggesting that there is a potential role for epigenetic modifications of *NRF2* in human prostate cancer (8, 36). However, there are no data showing the molecular mechanisms behind the epigenetic regulation of *NRF2*. Previous studies have reported the downregulation of GSTP1, RARβ, TNFRSF10C, RASSF1A, and *Neurog1* by epigenetic modifications and the presence of many other methylation markers in human prostate cancer (5, 6, 40). In this study, we

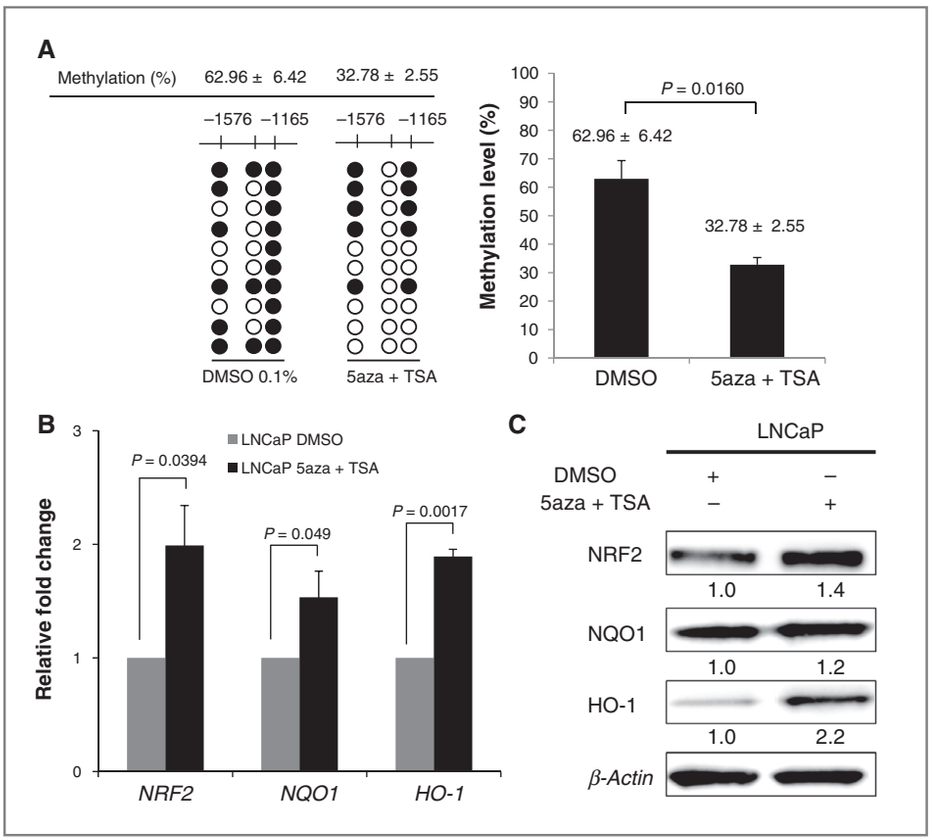

Figure 4. 5-aza/TSA–treated LNCaP cells decreased the methylation level of three CpGs sites of *NRF2* promoter and restored the expression of NRF2 and ARE-mediated genes. LNCaP cells were treated with DMSO 0.1% or combination of 5-aza/TSA (2.5 and 0.5 μmol/L, respectively) during 7 days. A, methylation level of three CpGs sites of *NRF2* promoter in LNCaP cells. Plasmid DNA from at least 10 colonies from each treatment was prepared using the QIAprep Spin Miniprep Kit (Qiagen) and sequenced (Genwiz). The white dots represent unmethylated and the black dots represent methylated CpG sites. Detailed procedure and sequence information are described in Material and Methods. The values are mean ± SD of three independent experiments. B, relative fold changes of mRNA expressions of *NRF2*, *NQO1*, and *HO-1* in LNCaP cell line were determined using quantitative real-time PCR (qPCR). Normalization of gene expression data was performed using *GAPDH* as internal control. RNAs were extracted from three independent experiments and analyzed using ABI7900HT qPCR system. Data are expressed as mean ± SD. Primer sequences are shown in Supplementary Table S1. C, protein level of NRF2, NQO1, and HO-1 in LNCaP cells. Protein expression level was normalized with *β-actin*. Images were analyzed by using ImageJ software (NIH; http://rsbweb.nih.gov/ij/). The different sources of the antibodies are described in Material and Methods.

present data demonstrating that *NRF2* is epigenetically regulated through promoter DNA methylation at three specific CpG sites, which were differentially hypermethylated in clinical prostate cancer tissues and human LNCaP cells and significantly decreased in BPH tissues (Figs. 1B, 2A, and 4A). Our IHC analysis of NRF2 expression in prostate tissues (moderate staining, with accumulated intensity value scored as 2+) showed that the accumulated intensity and the percentage of positive cells decreased progressively from normal prostate to adenocarcinoma tissues (adenocarcinoma tissue with Gleason score from 3–9; Fig. 2B and C). We also found that tumor tissues presented adjacent benign or normal lumina tissues that exhibited higher staining of NRF2 compared with the adenocarcinoma cells (Fig. 2B). Importantly, the expression of *NRF2* in human prostate cancer has been shown to be significantly reduced in advanced-stage tumors compared with normal prostate in several published human cancer gene expression datasets (ONCOMINE; ref. 41), providing evidence that DNA methylation of the *NRF2* promoter could contribute to regulation of transcription activity of *NRF2* in advanced stage of human prostate cancer (Supplementary Fig. S3; refs. 42–48).

The functional role of the DNA methylation of the three specific CpG sites in the CpG island of *NRF2* was assessed through luciferase reporter constructs and *in vitro* methylation assays (Fig. 3). The designed pGL-4.15–1169 and pGL-4.15–1526 reporters were active in LNCaP, PC-3, and HeLa cell lines, as shown in Fig. 3C and Supplementary Fig. S2. Interestingly, the promoter sequence containing the three CpG sites from −1526 to −1169 in LNCaP cells repressed the transcriptional activity of the *NRF2* promoter when methylated *in vitro* by CpG methyltransferase (Fig. 3C). Furthermore, this DNA sequence was able to interact with specific repressive factors revealed by ChIP assay analysis (Fig. 6). Interestingly, we have computationally identified seven putative transcription factor–binding

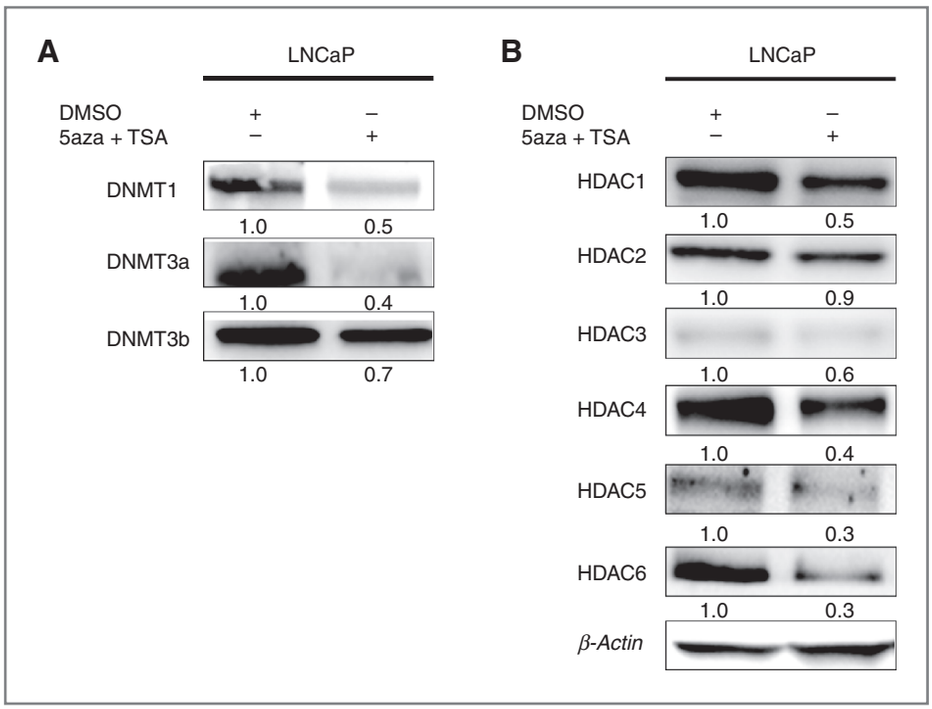

Figure 5. 5-aza/TSA–treated LNCaP cells inhibited DNMTs/HDACs activity. LNCaP cells were treated with DMSO 0.1% or combination of 5-aza/TSA (2.5 and 0.5 μmol/L, respectively) during 7 days. A, protein levels of DNMTs (1, 3a, and 3b) enzymes in LNCaP cells. B, protein levels of HDACs (1–6) enzymes in LNCaP cells. Protein expression level was normalized with *β-actin*. Images were analyzed by using ImageJ software (NIH; http://rsbweb.nih.gov/ij/). The different sources of the antibodies are described in Material and Methods.

sites (TFBS) in the genomic sequence of human *NRF2* promoter region comprising two out of the three relevant CpG site (Supplementary Fig. S4). Accordingly, the TFBS identified for the first CpG site were: NF-1 (neurofibromin 1), FOXP3 (forkhead box P3), *Pax-5* (paired box 5), and p53 (tumor protein p53); and for the second CpG site: GR-α (glucocorticoid receptor), c-Ets-1 (v-ets avian erythroblastosis virus E26 oncogene homolog 1), and c-Ets-2 (v-ets avian erythroblastosis virus E26 oncogene homolog 2). These observations suggest that these three specific CpG sites could be potentially relevant in the methylation-dependent suppression of *NRF2* expression *in vitro*. Similarly, we described the methylation activity of five specific CpGs sites in TRAMP C1 cells, which controls the transcriptional activity of *Nrf2* through the interaction with MBDs and histone modifications (8). Interestingly, we also demonstrated that these epigenetic mechanisms regulating *NRF2* expression in prostate cancer TRAMP mice can be reversed by dietary phytochemicals, thereby revealing that specific CpG hypermethylation of the *NRF2* promoter

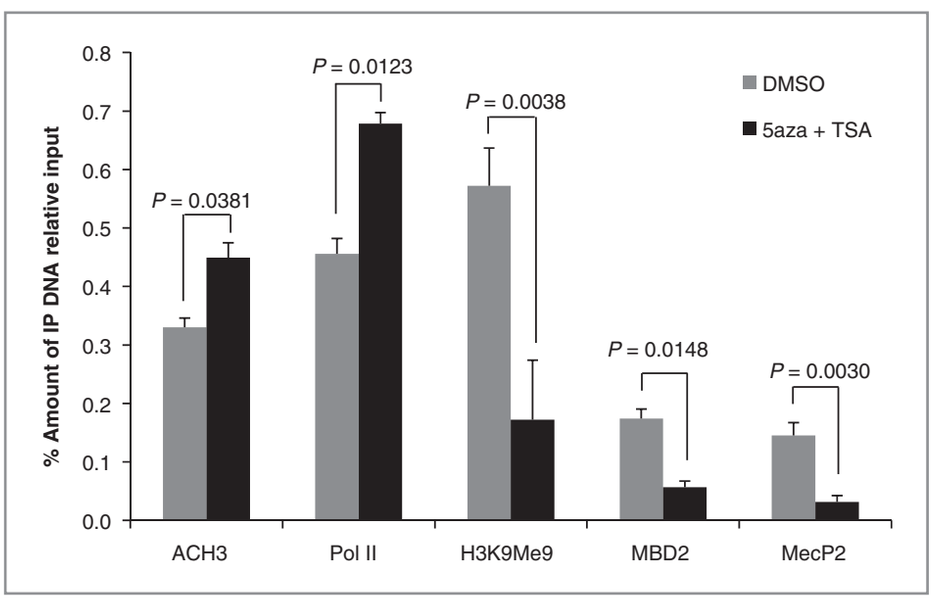

Figure 6. Hypermethylated CpG sites were associated with H3K9m3 and histone modification, which can be reversed by 5-aza/TSA treatment. LNCaP cells were treated with DMSO and 5-aza/TSA for 7 days, ChIP assay was performed to pull down the DNA-bound protein complexes using anti-AcH3, anti-Pol II, anti-H3K9m3, anti-MBD2, and anti-MecP2 antibodies. The results from three independent experiments were quantified on the basis of comparison with the inputs by qPCR. The values are mean ± SD. Primer sequences were designed covering a 93-bp fragment that is 29 bp upstream of the first CpG site in the *NRF2* promoter (Supplementary Table S1).

could represent a potential molecular biomarker for human prostate cancer prevention (4, 36, 49).

Several studies have revealed that the methylation of CpG sites in gene promoters is a frequent cause of epigenetic gene silencing in prostate cancer cell lines and can be reversed by using DNMT and HDAC inhibitors (5, 50–52). To interrogate the role of epigenetic modifications in the suppression of NRF2 expression and its activation, we treated LNCaP cells with the DNMT and HDAC inhibitors 5-aza and TSA, respectively. The results from this study revealed that the expression of NRF2 and the downstream NQO1 and HO-1 proteins was restored after the 5-aza/TSA treatment (Fig. 4B and C). Our previous observations in prostate cancer TRAMP mice and TRAMP C1 cells confirmed that methylation is important for the regulation of *NRF2* expression and that the treatment of TRAMP C1 cells with the DNMT/HDAC inhibitors 5-aza/TSA and dietary phytochemicals, such as curcumin and sulforaphane, restore the expression of NRF2 and induce downstream genes, such as NQO1 (8, 21, 53). Thus, the reactivation of NRF2 in LNCaP cells was consistent with the decreased methylation status and protein expression levels of DNMT1, DNMT3a, and DNMT3b (Fig. 5A).

In this study, we performed ChIP assays to explore the molecular mechanisms underlying the suppression of *NRF2* via methylation of the three specific promoter CpG sites. The results showed that 5-aza/TSA–treated LNCaP cells enriched the total amount of RNA Pol II and H3Ac and further decreased the total amount of H3-Lys9 (H3K9me3), MBD2, and MeCP2 at the CpG sites of the *NRF2* promoter (Fig. 6), which correlates well with the reexpression of NRF2 and decreased methylation levels (Fig. 4A–C). These observations are in agreement with previous studies in which 5-aza and TSA treatments are able to modulate the methylation-dependent association of various MBDs, such as MBD1–MBD4 and MeCP2, and the interaction of these proteins with a corepressor complex that includes HDACs (34). Ultimately, this process results in gene transcriptional repression (32–34). In previous studies using the same molecular approach in prostate tumors from TRAMP mice, we demonstrated that CpG methylation of the *Nrf2* promoter was associated with MBD2, H3Ac, and H3-Lys9 (H3K9me3; ref. 8). Similarly, in LNCaP cells, we found that the MBD2 and MeCP2 proteins and the H3K27me3 epigenetic modification are involved in the transcriptional repression of *Neurog1* (40). The above results confirmed our findings in LNCaP cells showing that the enrichment of H3-Lys9 (H3K9me3), MBD2, and MeCP2 is related to transcriptionally repressed chromatin (54). These results are also supported by the increased protein expression of HDACs (HDACs 1–6) in DMSO-treated control LNCaP cells compared with 5-aza/TSA–treated cells (Fig. 5B).

In summary, this study shows for the first time that the *in vitro* hypermethylation of three specific CpG sites in the *NRF2* promoter correlates with reduced NRF2 expression in human prostate cancer cells and the hypermethylated status of the *NRF2* promoter in clinical prostate cancer tissues. These findings provide new insights into earlier observations that showed differential NRF2 expression in human prostate tumors (20). Further studies of the methylation profiles from a large number of primary tumor samples will provide important information on the role of methylation of the CpG islands in the *NRF2* promoter. Importantly, the *NRF2* methylation status may contribute to regulation of transcription activity of *NRF2*, which could be used as preventive and therapeutic target for the treatment of prostate cancer in future clinical trials.

Disclosure of Potential Conflicts of Interest

No potential conflicts of interest were disclosed.

Authors' Contributions

Conception and design: T.O. Khor, F. Fuentes, S. Yegnasubramanian, A.-N.T. Kong
Development of methodology: T.O. Khor, F. Fuentes, A.Y. Yang, Y. Liu, D.J. Smiraglia, A.-N.T. Kong
Acquisition of data (provided animals, acquired and managed patients, provided facilities, etc.): F. Fuentes, L. Shu, X. Paredes-Gonzalez, A.Y. Yang, Y. Liu, D.J. Smiraglia, A.-N.T. Kong
Analysis and interpretation of data (e.g., statistical analysis, biostatistics, computational analysis): F. Fuentes, L. Shu, X. Paredes-Gonzalez, D.J. Smiraglia, W.G. Nelson, A.-N.T. Kong
Writing, review, and/or revision of the manuscript: T.O. Khor, F. Fuentes, D.J. Smiraglia, S. Yegnasubramanian, W.G. Nelson, A.-N.T. Kong
Administrative, technical, or material support (i.e., reporting or organizing data, constructing databases): F. Fuentes, A.-N.T. Kong
Study supervision: T.O. Khor, F. Fuentes, A.-N.T. Kong

Acknowledgments

The authors thank all the members in A.-N.T. Kong's laboratory for their helpful discussion and preparation of this article.

Grant Support

This work was supported, in part, by institutional funds and by R01-CA118947, R01-CA152826, from the National Cancer Institute (NCI), R01AT007065 from the National Center for Complementary and Alternative Medicines (NCCAM) and the Office of Dietary Supplements (ODS; to A.-N. T. Kong).

The costs of publication of this article were defrayed in part by the payment of page charges. This article must therefore be hereby marked *advertisement* in accordance with 18 U.S.C. Section 1734 solely to indicate this fact.

Received April 14, 2014; revised August 27, 2014; accepted September 16, 2014; published OnlineFirst September 29, 2014.

References

1. Cary KC, Cooperberg MR. Biomarkers in prostate cancer surveillance and screening: past, present, and future. Ther Adv Urol 2013;5:318–29.
2. Siegel R, Ma J, Zou Z, Jemal A. Cancer statistics, 2014. CA Cancer J Clin 2014;64:9–29.
3. Aryee MJ, Liu W, Engelmann JC, Nuhn P, Gurel M, Haffner MC, et al. DNA methylation alterations exhibit intraindividual stability and interindividual heterogeneity in prostate cancer metastases. Sci Transl Med 2013;5:169ra10.
4. Lee JH, Khor TO, Shu L, Su ZY, Fuentes F, Kong AN. Dietary phytochemicals and cancer prevention: Nrf2 signaling, epigenetics, and cell death mechanisms in blocking cancer initiation and progression. Pharmacol Ther 2013;137:153–71.

5. Majumdar S, Buckles E, Estrada J, Koochekpour S. Aberrant DNA methylation and prostate cancer. Curr Genomics 2011;12: 486–505.
6. Ahmed H. Promoter methylation in prostate cancer and its application for the early detection of prostate cancer using serum and urine samples. Biomark Cancer 2010;2:17–33.
7. Perry AS, Foley R, Woodson K, Lawler M. The emerging roles of DNA methylation in the clinical management of prostate cancer. Endocr Relat Cancer 2006;13:357–77.
8. Yu S, Khor TO, Cheung KL, Li W, Wu TY, Huang Y, et al. Nrf2 expression is regulated by epigenetic mechanisms in prostate cancer of TRAMP mice. PLoS ONE 2010;5:e8579.
9. Yu S, Kong AN. Targeting carcinogen metabolism by dietary cancer preventive compounds. Curr Cancer Drug Targets 2007;7:416–24.
10. Kong AN, Yu R, Lei W, Mandlekar S, Tan TH, Ucker DS. Differential activation of MAPK and ICE/Ced-3 protease in chemical-induced apoptosis. The role of oxidative stress in the regulation of mitogen-activated protein kinases (MAPKs) leading to gene expression and survival or activation of caspases leading to apoptosis. Restor Neurol Neurosci 1998;12:63–70.
11. Kwak MK, Itoh K, Yamamoto M, Sutter TR, Kensler TW. Role of transcription factor Nrf2 in the induction of hepatic phase 2 and antioxidative enzymes *in vivo* by the cancer chemoprotective agent, 3H-1, 2-dimethiole-3-thione. Mol Med 2001;7:135–45.
12. Chan K, Lu R, Chang JC, Kan YW. NRF2, a member of the NFE2 family of transcription factors, is not essential for murine erythropoiesis, growth, and development. Proc Natl Acad Sci U S A 1996;93: 13943–8.
13. Suzuki T, Motohashi H, Yamamoto M. Toward clinical application of the Keap1–Nrf2 pathway. Trends Pharmacol Sci 2013;34:340–6.
14. Ramos-Gomez M, Kwak MK, Dolan PM, Itoh K, Yamamoto M, Talalay P, et al. Sensitivity to carcinogenesis is increased and chemoprotective efficacy of enzyme inducers is lost in nrf2 transcription factor-deficient mice. Proc Natl Acad Sci U S A 2001;98:3410–5.
15. Fahey JW, Haristoy X, Dolan PM, Kensler TW, Scholtus I, Stephenson KK, et al. Sulforaphane inhibits extracellular, intracellular, and antibiotic-resistant strains of Helicobacter pylori and prevents benzo[a]pyrene-induced stomach tumors. Proc Natl Acad Sci U S A 2002;99:7610–5.
16. Khor TO, Huang MT, Prawan A, Liu Y, Hao X, Yu S, et al. Increased susceptibility of Nrf2 knockout mice to colitis-associated colorectal cancer. Cancer Prev Res 2008;1:187–91.
17. Saw CL, Huang MT, Liu Y, Khor TO, Conney AH, Kong AN. Impact of Nrf2 on UVB-induced skin inflammation/photoprotection and photoprotective effect of sulforaphane. Mol Carcinog 2011;50:479–86.
18. Xu C, Huang MT, Shen G, Yuan X, Lin W, Khor TO, et al. Inhibition of 7,12-dimethylbenz(a)anthracene-induced skin tumorigenesis in C57BL/6 mice by sulforaphane is mediated by nuclear factor E2-related factor 2. Cancer Res 2006;66:8293–6.
19. Khor TO, Huang MT, Kwon KH, Chan JY, Reddy BS, Kong AN. Nrf2-deficient mice have an increased susceptibility to dextran sulfate sodium-induced colitis. Cancer Res 2006;66:11580–4.
20. Frohlich DA, McCabe MT, Arnold RS, Day ML. The role of Nrf2 in increased reactive oxygen species and DNA damage in prostate tumorigenesis. Oncogene 2008;27:4353–62.
21. Khor TO, Huang Y, Wu TY, Shu L, Lee J, Kong AN. Pharmacodynamics of curcumin as DNA hypomethylation agent in restoring the expression of Nrf2 via promoter CpGs demethylation. Biochem Pharmacol 2011;82:1073–8.
22. Nakayama M, Gonzalgo ML, Yegnasubramanian S, Lin X, De Marzo AM, Nelson WG. GSTP1 CpG island hypermethylation as a molecular biomarker for prostate cancer. J Cell Biochem 2004;91: 540–52.
23. Bostwick DG, Meiers I, Shanks JH. Glutathione *S*-transferase: differential expression of alpha, mu, and pi isoenzymes in benign prostate, prostatic intraepithelial neoplasia, and prostatic adenocarcinoma. Hum Pathol 2007;38:1394–401.
24. Kotrikadze N, Alibegashvili M, Zibzibadze M, Abashidze N, Chigogidze T, Managadze L, et al. Activity and content of antioxidant enzymes in prostate tumors. Exp Oncol 2008;30:244–7.
25. Mohler JL, Gregory CW, Ford OH III, Kim D, Weaver CM, Petrusz P, et al. The androgen axis in recurrent prostate cancer. Clin Cancer Res 2004;10:440–8.
26. Berthon P, Dimitrov T, Stower M, Cussenot O, Maitland NJ. A microdissection approach to detect molecular markers during progression of prostate cancer. Br J Cancer 1995;72:946–51.
27. Ghosh S, Yates AJ, Fruhwald MC, Miecznikowski JC, Plass C, Smiraglia D. Tissue specific DNA methylation of CpG islands in normal human adult somatic tissues distinguishes neural from non-neural tissues. Epigenetics 2010;5:527–38.
28. Li LC, Dahiya R. MethPrimer: designing primers for methylation PCRs. Bioinformatics 2002;18:1427–31.
29. Fuentes F, Shu L, Lee JH, Su Z-Y, Lee K-R, Kong A-NT. Nrf2-target approaches in cancer chemoprevention mediated by dietary phytochemicals. In: Bode AM, Dong Z, editors. Cancer prevention. Methods in pharmacology and toxicology: New York: Springer; 2014. p. 53–83.
30. Lee JH, Lee KR, Su ZY, Boyanapalli SS, Barman DN, Huang MT, et al. *In vitro* and *in vivo* anti-inflammatory effects of a novel 4,6-bis ((E)-4-hydroxy-3-methoxystyryl)-1-phenethylpyrimidine-2(1H)-thione. Chem Res Toxicol 2014;27:34–41.
31. Takai D, Jones PA. The CpG island searcher: a new WWW resource. In Silico Biol 2003;3:235–40.
32. Hendrich B, Bird A. Identification and characterization of a family of mammalian methyl-CpG binding proteins. Mol Cell Biol 1998;18: 6538–47.
33. Lewis JD, Meehan RR, Henzel WJ, Maurer-Fogy I, Jeppesen P, Klein F, et al. Purification, sequence, and cellular localization of a novel chromosomal protein that binds to methylated DNA. Cell 1992;69:905–14.
34. Nan X, Ng HH, Johnson CA, Laherty CD, Turner BM, Eisenman RN, et al. Transcriptional repression by the methyl-CpG–binding protein MeCP2 involves a histone deacetylase complex. Nature 1998;393: 386–9.
35. He X, Lin GX, Chen MG, Zhang JX, Ma Q. Protection against chromium (VI)–induced oxidative stress and apoptosis by Nrf2. Recruiting Nrf2 into the nucleus and disrupting the nuclear Nrf2/Keap1 association. Toxicol Sci 2007;98:298–309.
36. Wu TY, Khor TO, Su ZY, Saw CL, Shu L, Cheung KL, et al. Epigenetic modifications of Nrf2 by 3,3′-diindolylmethane *in vitro* in TRAMP C1 cell line and *in vivo* TRAMP prostate tumors. AAPS J 2013;15:864–74.
37. Sporn MB, Liby KT. NRF2 and cancer: the good, the bad and the importance of context. Nat Rev Cancer 2012;12:564–71.
38. Lister A, Nedjadi T, Kitteringham NR, Campbell F, Costello E, Lloyd B, et al. Nrf2 is overexpressed in pancreatic cancer: implications for cell proliferation and therapy. Mol Cancer 2011;10:37.
39. Niture SK, Khatri R, Jaiswal AK. Regulation of Nrf2—an update. Free Radic Biol Med 2014;66:36–44.
40. Shu L, Khor TO, Lee JH, Boyanapalli SS, Huang Y, Wu TY, et al. Epigenetic CpG demethylation of the promoter and reactivation of the expression of Neurog1 by curcumin in prostate LNCaP cells. AAPS J 2011;13:606–14.
41. Rhodes DR, Yu J, Shanker K, Deshpande N, Varambally R, Ghosh D, et al. ONCOMINE: a cancer microarray database and integrated data-mining platform. Neoplasia 2004;6:1–6.
42. Varambally S, Yu J, Laxman B, Rhodes DR, Mehra R, Tomlins SA, et al. Integrative genomic and proteomic analysis of prostate cancer reveals signatures of metastatic progression. Cancer Cell 2005;8:393–406.
43. Luo J, Duggan DJ, Chen Y, Sauvageot J, Ewing CM, Bittner ML, et al. Human prostate cancer and benign prostatic hyperplasia: molecular dissection by gene expression profiling. Cancer Res 2001;61:4683–8.
44. Holzbeierlein J, Lal P, LaTulippe E, Smith A, Satagopan J, Zhang L, et al. Gene expression analysis of human prostate carcinoma during hormonal therapy identifies androgen-responsive genes and mechanisms of therapy resistance. Am J Pathol 2004;164:217–27.
45. Taylor BS, Schultz N, Hieronymus H, Gopalan A, Xiao Y, Carver BS, et al. Integrative genomic profiling of human prostate cancer. Cancer Cell 2010;18:11–22.
46. Wallace TA, Prueitt RL, Yi M, Howe TM, Gillespie JW, Yfantis HG, et al. Tumor immunobiological differences in prostate cancer between African-American and European-American men. Cancer Res 2008;68: 927–36.

47. Liu P, Ramachandran S, AliSeyed M, Scharer CD, Laycock N, Dalton WB, et al. Sex-determining region Y box 4 is a transforming oncogene in human prostate cancer cells. Cancer Res 2006;66:4011–9.
48. Lapointe J, Li C, Higgins JP, vande Rijn M, Bair E, Montgomery K, et al. Gene expression profiling identifies clinically relevant subtypes of prostate cancer. Proc Natl Acad Sci U S A 2004;101:811–6.
49. Su ZY, Khor TO, Shu L, Lee JH, Saw CL, Wu TY, et al. Epigenetic reactivation of Nrf2 in murine prostate cancer TRAMP C1 cells by natural phytochemicals Z-ligustilide and Radix Angelica Sinensis via promoter CpG demethylation. Chem Res Toxicol 2013;26:477–85.
50. Kawamoto K, Okino ST, Place RF, Urakami S, Hirata H, Kikuno N, et al. Epigenetic modifications of RASSF1A gene through chromatin remodeling in prostate cancer. Clin Cancer Res 2007;13:2541–8.
51. Mavis CK, MoreyKinney SR, Foster BA, Karpf AR. Expression level and DNA methylation status of glutathione-*S*-transferase genes in normal murine prostate and TRAMP tumors. Prostate 2009;69: 1312–24.
52. Su ZY, Shu L, Khor TO, Lee JH, Fuentes F, Kong AN. A perspective on dietary phytochemicals and cancer chemoprevention: oxidative stress, Nrf2, and epigenomics. Top Curr Chem 2012;329:133–62.
53. Zhang C, Su ZY, Khor TO, Shu L, Kong AN. Sulforaphane enhances Nrf2 expression in prostate cancer TRAMP C1 cells through epigenetic regulation. Biochem Pharmacol 2013;85:1398–404.
54. Bannister AJ, Zegerman P, Partridge JF, Miska EA, Thomas JO, Allshire RC, et al. Selective recognition of methylated lysine 9 on histone H3 by the HP1 chromo domain. Nature 2001;410:120–4.